# Instability and transport phenomena in oscillating suspensions of non-Brownian particles in confined geometries

**Alejandro Adrián GARCÍA**

Doctoral thesis in cotutelle between

**Universidad de Buenos Aires**
Facultad de Ingeniería
Direction: Irene Ippolito
Co-direction: Y. Lucrecia Roht

**Université Paris-Saclay**
École doctorale SMEMaG
Direction: Georges Gauthier

# Suspension of particles

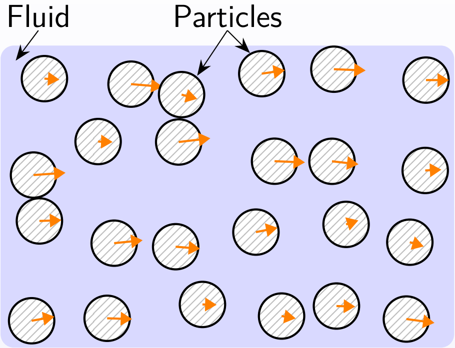


Two-phase system:
solid particles in a liquid.

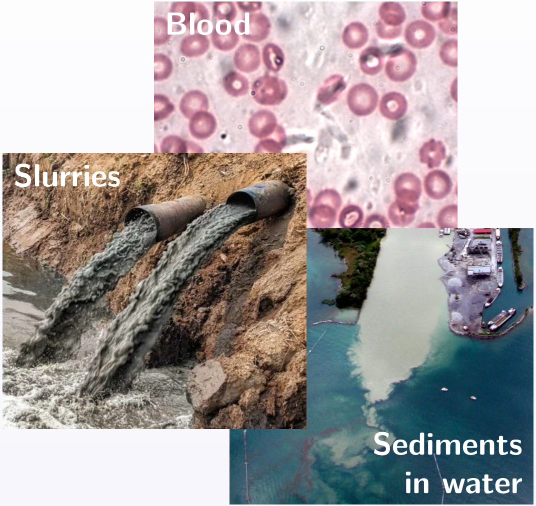

# Suspensions as effective fluids

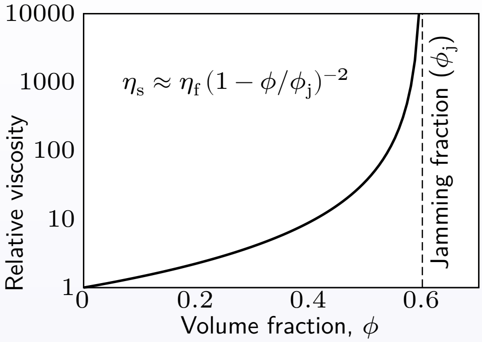


- Particle-fluid and particle-particle interactions contribute to the suspension stress.
- The suspension viscosity $\eta_s$ increases with the particle volume fraction $\phi$.
- Non-Newtonian: shear thinning and thickening, and normal stress differences.

Ref. Maron and Pierce (1956)

See also Guazzelli and Pouliquen (2018)

$$\phi = \frac{\text{Volume with particles}}{\text{Total volume}}$$

# Simple shear flows in the Stokes regime

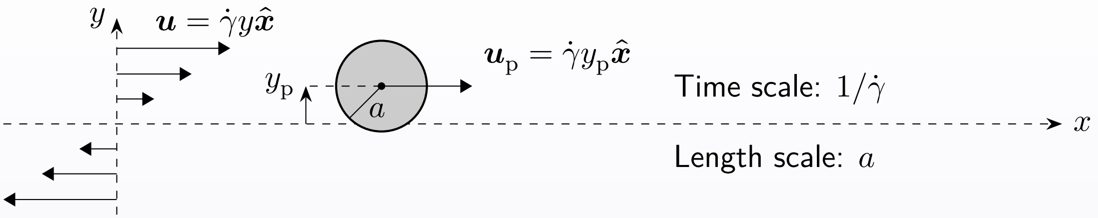


Time scale: $1/\dot{\gamma}$

Length scale: $a$

- $\mathrm{Re} = 0$. No inertia. All velocities result from balances of forces.
- Local fluid velocity $\boldsymbol{u}$ depends linearly on $y$ with a shear rate $\dot{\gamma}$.
- Laminar flows: locally a shear flow with $\dot{\gamma}$ varying with position.
- Force-free spheres move with the velocity corresponding to its center position.

# Particle pair interactions

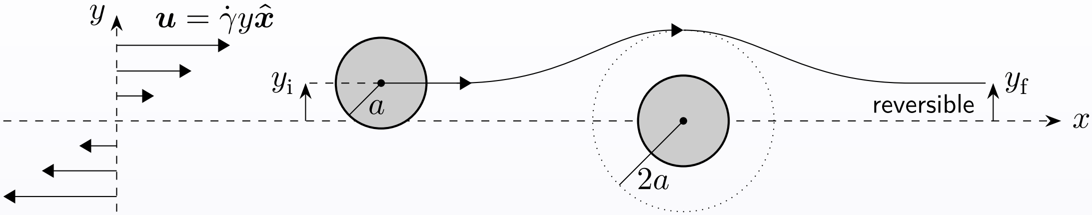


- Two particles in different streamlines can get very close and have strong interactions (i.e. a collision).
- Hydrodynamic interactions (mediated by the fluid) are reversible under shear reversal and the spheres return to their original streamlines ($y_{\mathrm{f}} = y_{\mathrm{i}}$).
- Other interactions may not have this property, in particular...

# Irreversible pair interactions

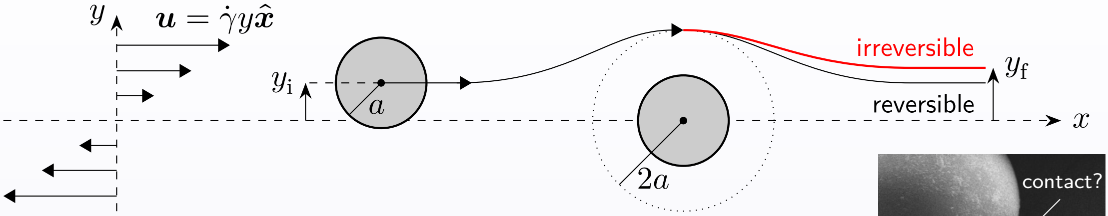


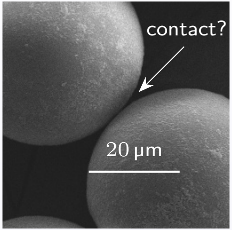


- Real spheres have rough surfaces. Asperity size $\sim 10^{-4}\,a$.
- Particle surfaces can approach enough to make contact.
- Contact forces prevent approach, but not separation: they are irreversible.
  $\rightarrow$ Irreversible trajectories ($y_\mathrm{f} > y_\mathrm{i}$).

# Irreversible behavior: diffusion and migration

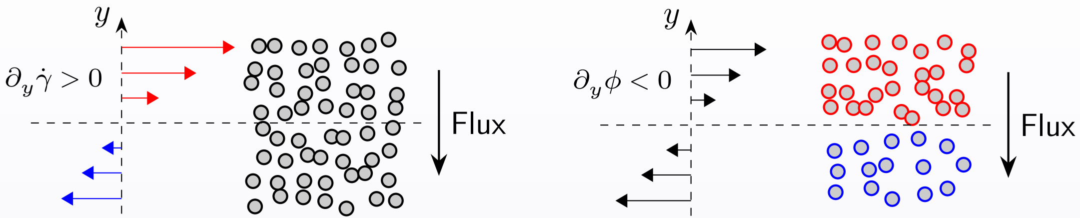


- Irreversible collisions → Particle self-diffusivity $D = \hat{D}(\phi)\,\dot\gamma a^2$, $\frac{\mathrm{d}\hat{D}}{\mathrm{d}\phi} > 0$.
- Shear-induced migration: particles tend to migrate following the descending gradients of $\dot\gamma$ and $\phi$.
- Non-uniform particle distribution and suspension properties (e.g. $\eta_s$).

# Previous work and motivation

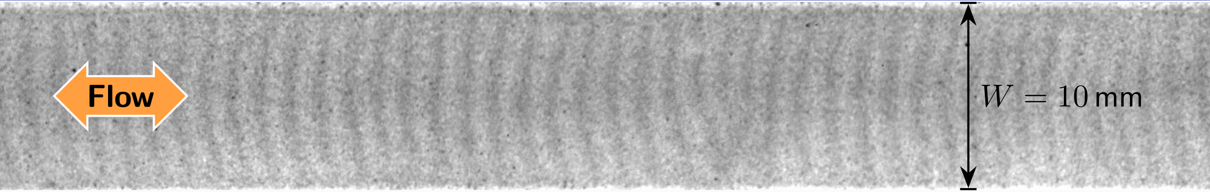


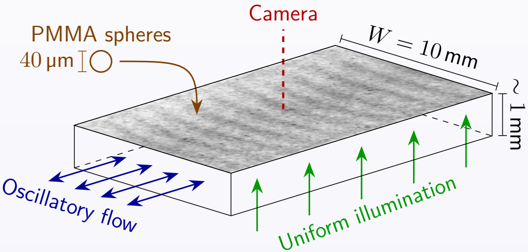


Image intensity $= f(\phi)$

Experiments by Roht et al. (EPL 2018):

- Suspension of spheres, $\phi_{\mathrm{bulk}} = 0.35$
- Oscillatory channel flow (amplitude $\gg$ particle size)
- $\mathrm{Re} < 1$, $\mathrm{Pe} \to \infty$

Stripes appear with the oscillations

*What is happening inside?*

# New experiments and objectives

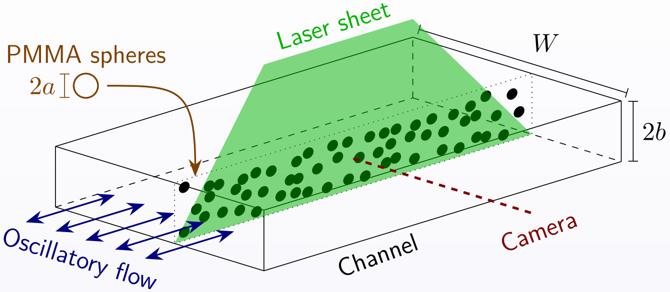


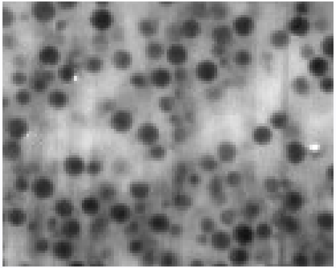

- Observe individual particles inside the channel.
- Determine the particle distribution and velocity field as the instability develops.
- Are particle trajectories reversible? How do they organize relative to each other?

# Visualization technique

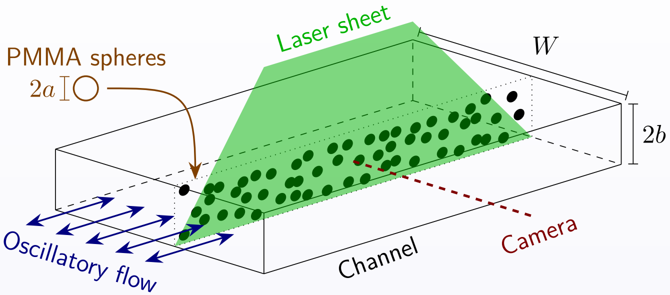


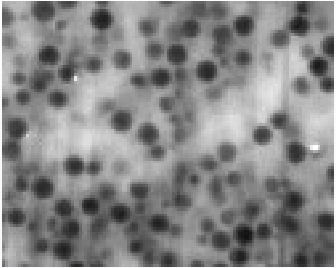

- Transparent suspension and channel.
  - PMMA (acrylic) spheres and channels.
  - Aqueous solutions as carrier fluids.
  - Index matching ($n_\mathrm{f} = n_\mathrm{p}$).
- Visualization using fluorescense.
  - One phase dyed (fluid or particles).
  - Illumination by a laser plane.
- Video analysis to track particles

# Suspensions used

- Monodisperse PMMA spheres.
  - Diameters $2a \approx 40$ and $85\,\mu\text{m}$.
  - "Large" size $\Rightarrow$ Non-Brownian, non-colloidal.
  - $0.2 \leq \phi_{\text{bulk}} \leq 0.4$
- Newtonian aqueous solutions.
  - Viscosities $\eta_{\text{f}} \approx 7.6$ (mostly) and $3000\,\text{mPa s}$.
  - Matching density ($\rho \approx 1.19\,\text{g/cm}^3$)
    $\Rightarrow$ Neutrally-buoyant particles.
  - Matching index of refraction ($n \approx 1.49$)
    $\Rightarrow$ Transparent suspensions.

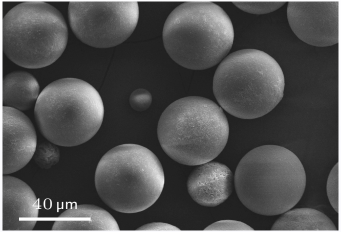


SEM image of $40\,\mu\text{m}$ particles.

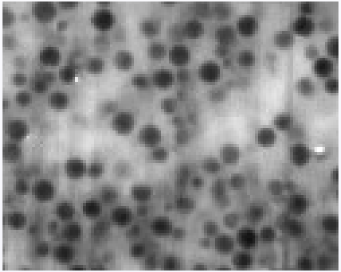

Suspension of $85\,\mu\text{m}$ particles illuminated by a light plane.

# Experimental setup

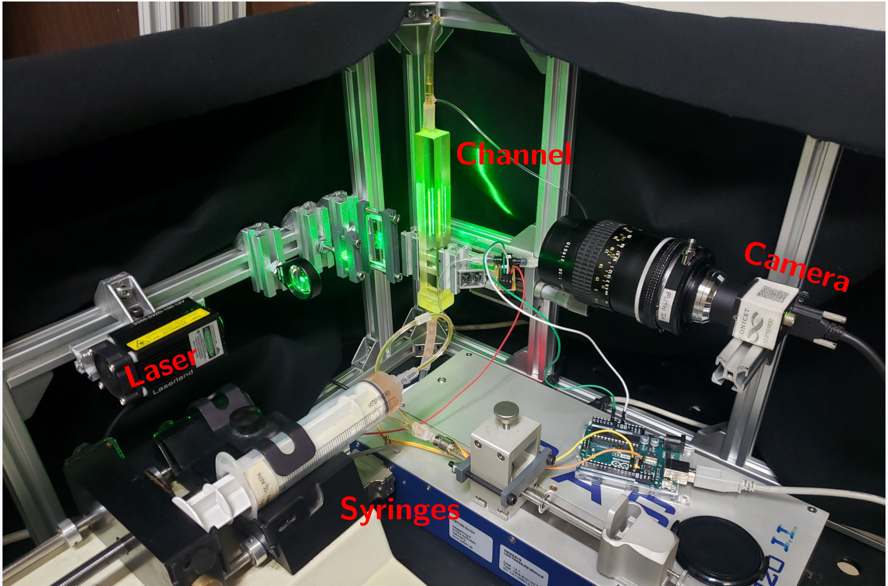

# Video of a typical experiment

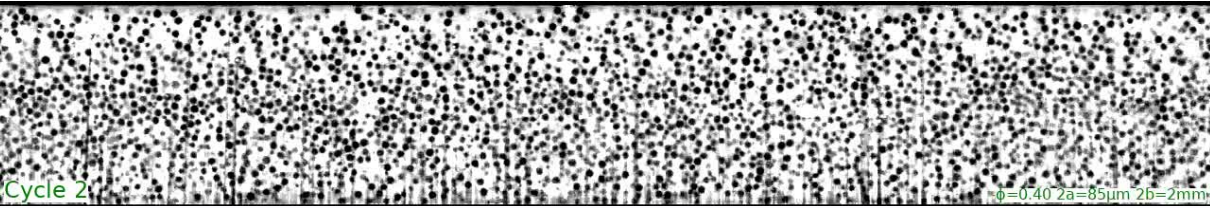


- White: fluorescent fluid.
- Black disks: spherical particles ($2a = 85\,\mu\text{m}$, $\phi_{\text{bulk}} = 0.4$).
- Channel thickness $2b = 2\,\text{mm}$.
- Square wave in the flow rate. Period $T = 8\,\text{s}$.
  Displacement amplitude $A = 4.5\,\text{mm}$.

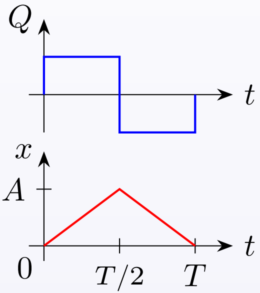

# A typical experiment in images

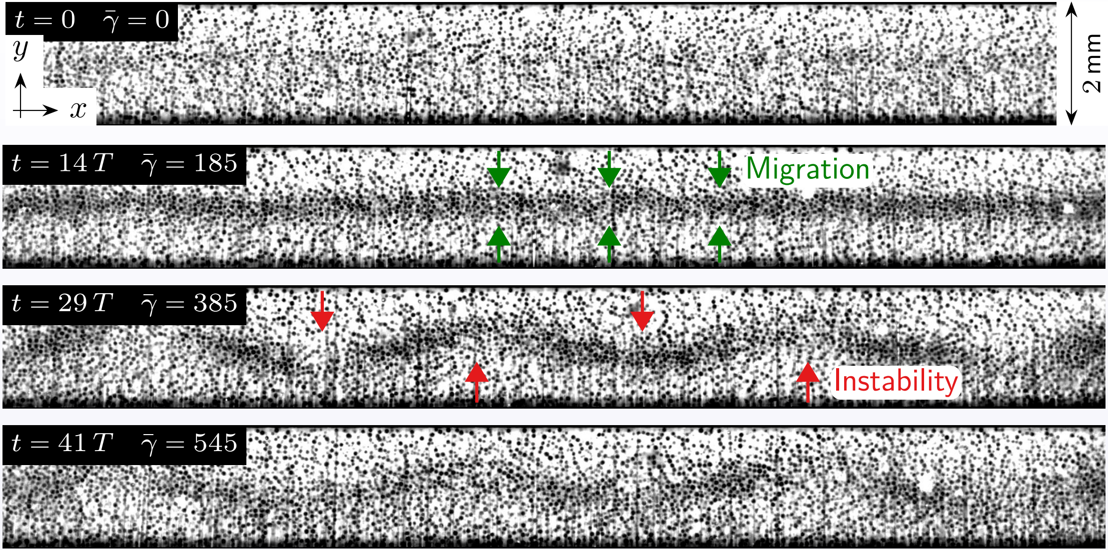

# Profiles after migration and before the instability

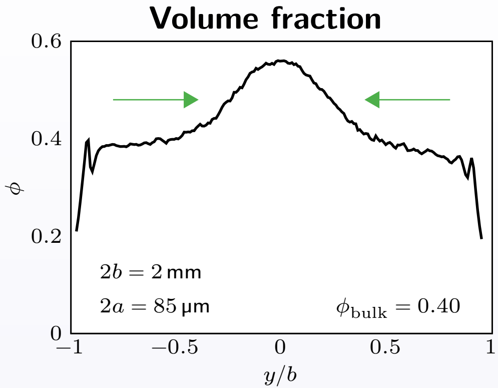


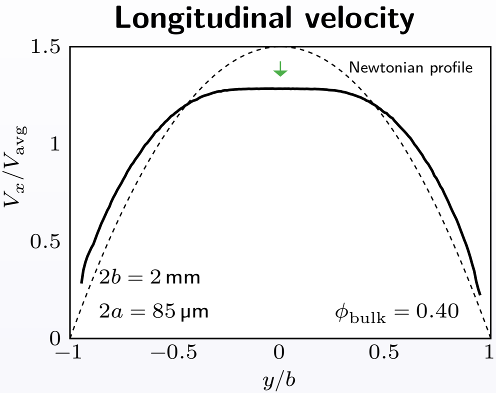


- Particles migrate from the walls ($y = \pm b$) toward the center ($y = 0$).
- In the center: more particles = larger viscosity.
- Flattened velocity profile.

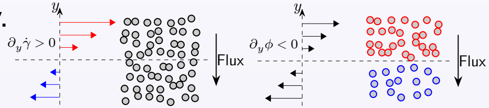

# Profiles after migration and before the instability

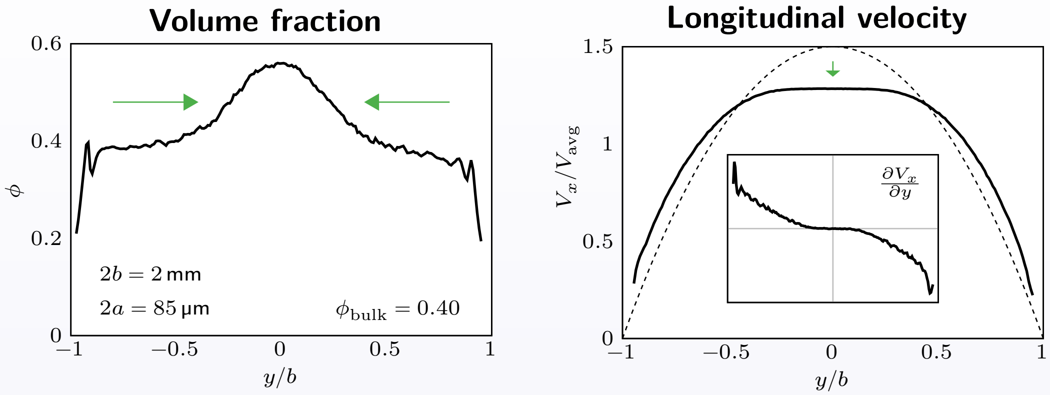


- **Shear rate** $\dot{\gamma} = \left|\frac{\partial V_x}{\partial y}\right|$ maximum near the walls. Nearly zero in the center.
- $1/\dot{\gamma}$ can be used as a local time scale.

# Transient effects of the flow reversals

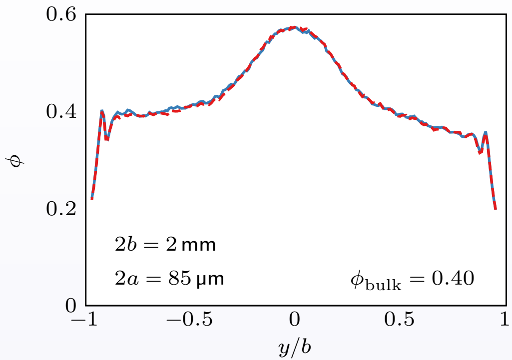


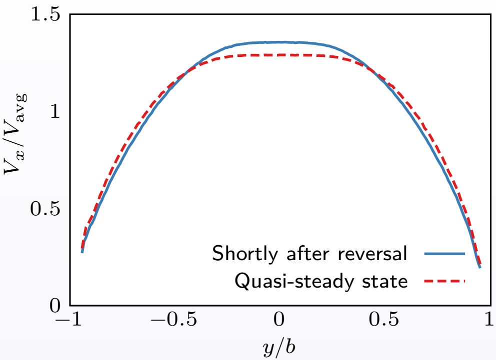


- After a flow reversal, the particles lose contacts.
- Non-uniform viscosity drop.
- Transient variation of the velocity profile $V_x(y)$.
- No variation of the volume fraction profile $\phi(y)$.

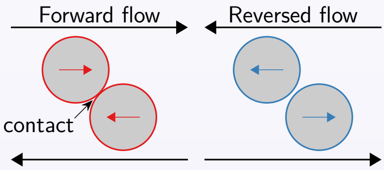

# Transient effects of the flow reversals

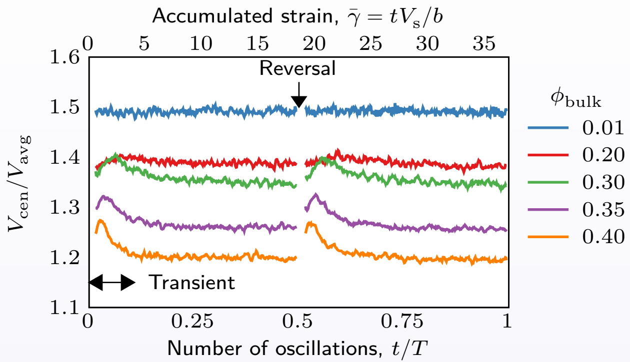


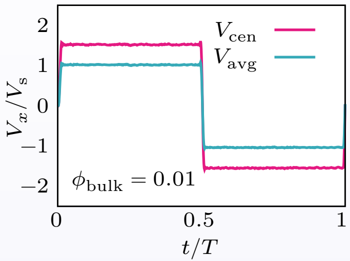


- Transient effects become more marked with increasing $\phi_{bulk}$.
- $tV_s$ = average accumulated travelled distance. $V_s \approx V_{avg}$.

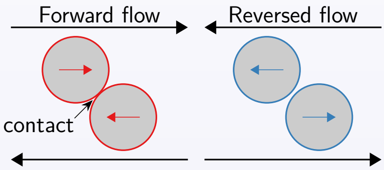

# Microstructure and pair distribution function

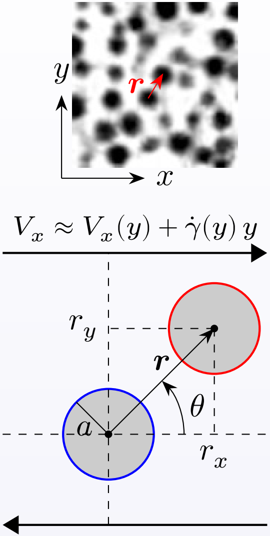


- We accumulate statistics of the relative positions $\boldsymbol{r}$ of particle pairs to obtain...
- $P(\boldsymbol{x}+\boldsymbol{r}|\boldsymbol{x})$ = probability of finding a particle at $\boldsymbol{x}+\boldsymbol{r}$ given another one at $\boldsymbol{x}$.
- Pair distribution function $g(\boldsymbol{r}) = P(\boldsymbol{x}+\boldsymbol{r}|\boldsymbol{x})/n$. Particle number density $n \propto \phi$.
- $g$ gives information about the particle microstructure separately of $\phi$.
- $\phi$, $\dot{\gamma}$, $g$ vary across the thickness ($y$ coordinate).

# PDF far from the walls and the center

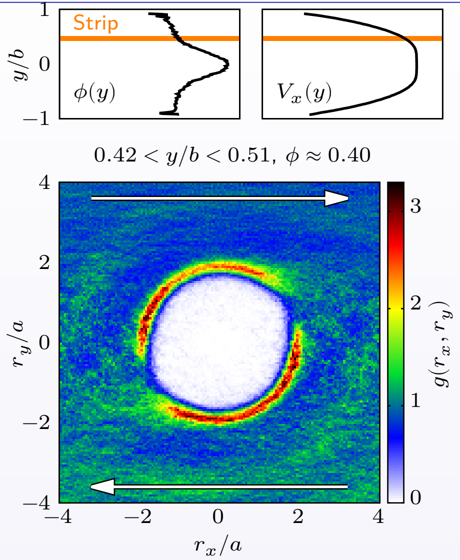


- In a narrow strip with $\phi$ and $\dot{\gamma} \approx$ uniform.
- 2D: all considered particles have their centers in the same $xy$ plane.
- Quasi-steady state (long enough after reversal).
- White disk: nil probability of pairs with $r \lesssim 2a$ (no interpenetration).
- Maximum probability for $r \approx 2a$ (red ring).

# PDF far from the walls and the center

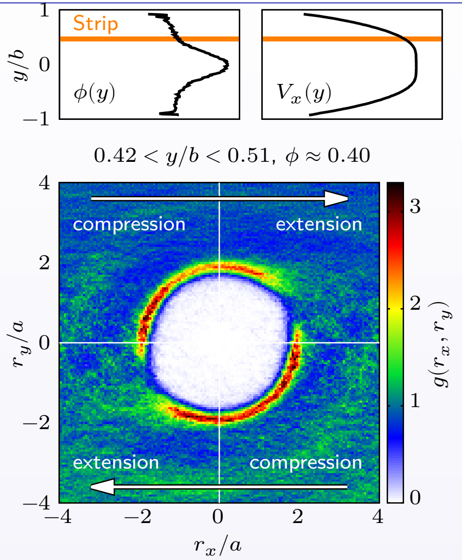


- Most particle pairs are nearly in contact ($r \approx 2a$).
- Most of them are in compression ($r_x r_y < 0$).
- Depletion of pairs in the extensional quadrant ($r_x r_y > 0$).
- Fore-aft asymmetric PDF due to irreversible interactions (contacts).

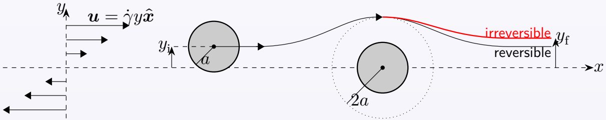

# Agreement with experiments using uniform shear flows

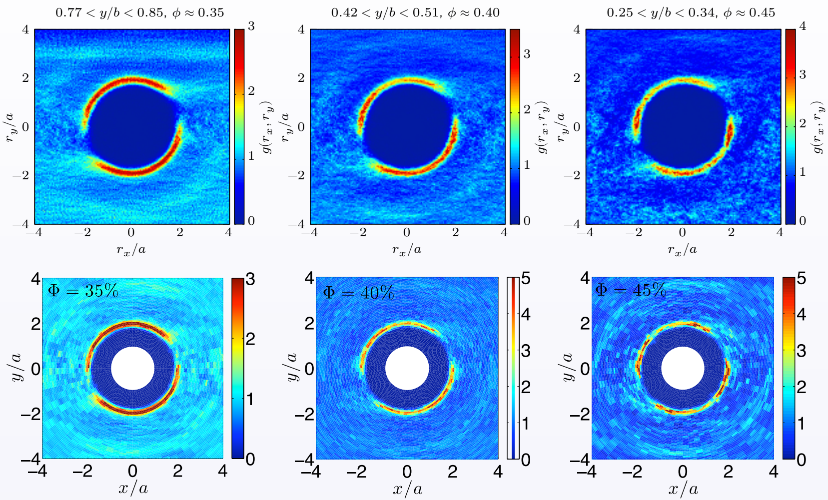


Same experiment, different positions $y$.

Different experiments with uniform $\phi$ and $\dot{\gamma}$. Blanc et al. (2013 J.Rheol.)

- The steady microstructure depends mostly on the local $\phi$.

# Reorganization after a flow reversal

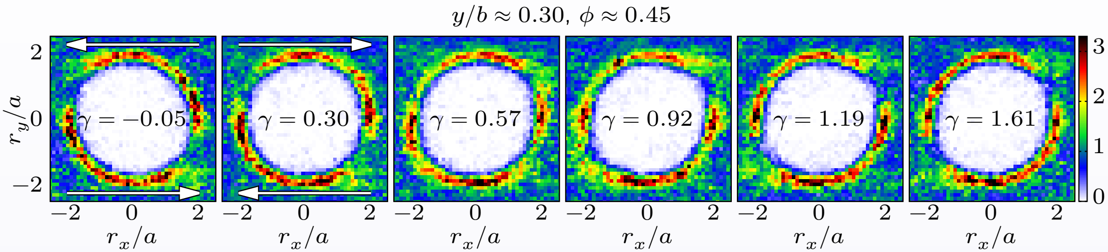


- The anisotropic microstructure depends on the shear direction.
- It must reorganize upon flow reversal.

$$\gamma(y, \Delta t) = \int_0^{\Delta t} \dot{\gamma}(y, t')\ \mathrm{d}t' = \text{accumulated local deformation after each reversal}$$

# Microstructure anisotropy parameter

$$A_{xy} = \left\langle \frac{r_x r_y}{r_x^2 + r_y^2} \right\rangle_{r \approx 2a}$$

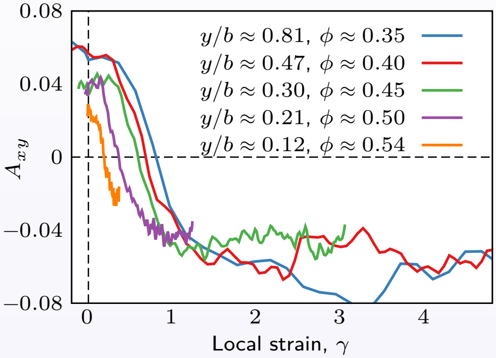


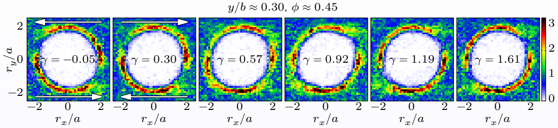


- $A_{xy}$ is one component of a 2D fabric tensor (Gillissen and Wilson 2018).
- $A_{xy}$ changes sign uppon shear reversal.
- The characteristic strain decreases with increasing $\phi$.

# Non-uniformity of the variations after a flow reversal

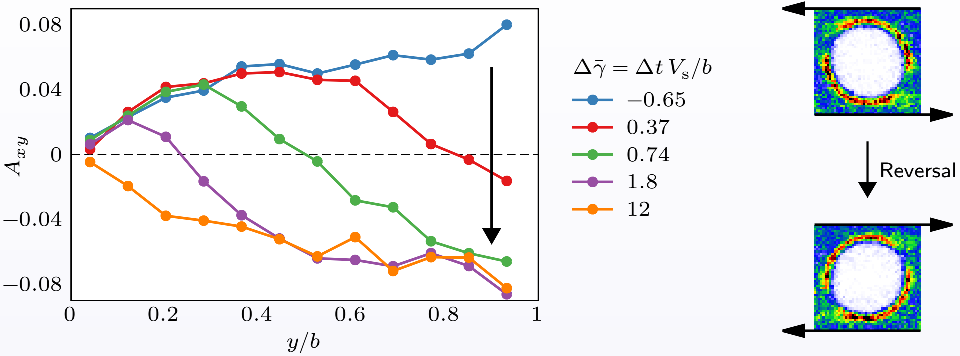


- Higher $\phi$ toward the center $(y = 0) \Rightarrow$ Smaller characteristic strains.
- Higher $\dot{\gamma}$ toward the walls $(y = b) \Rightarrow$ Faster accumulation of strain.
- Non-uniform variation of the suspension properties after each reversal.
  *Could it be related to the instability?*

# Flow instability induced by oscillations

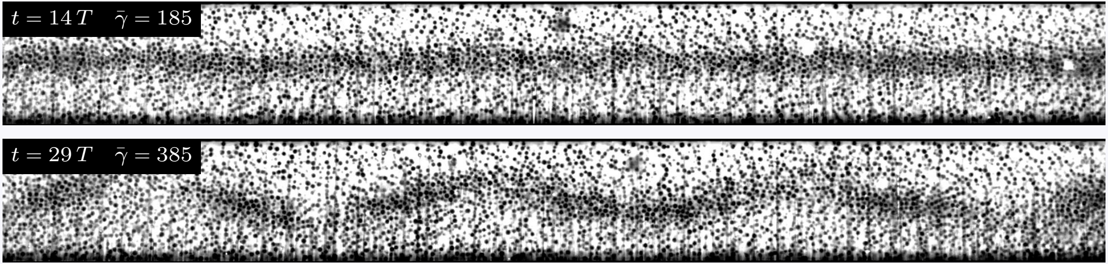

# Volume fraction and velocity fields in the $xy$ plane

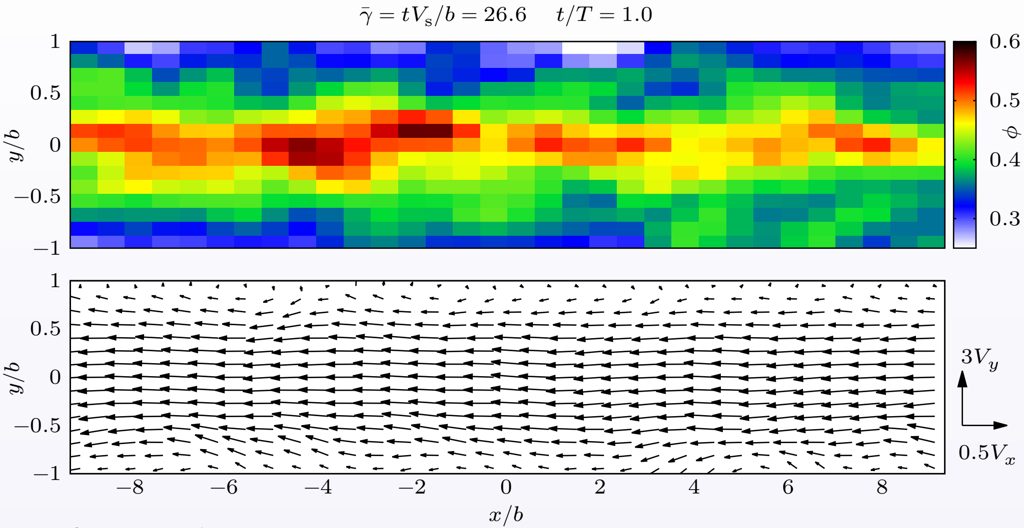


$2a = 85\,\mu\mathrm{m} \quad 2b = 2\,\mathrm{mm} \quad \phi_{\mathrm{bulk}} = 0.4$

# Volume fraction and velocity fields in the $xy$ plane

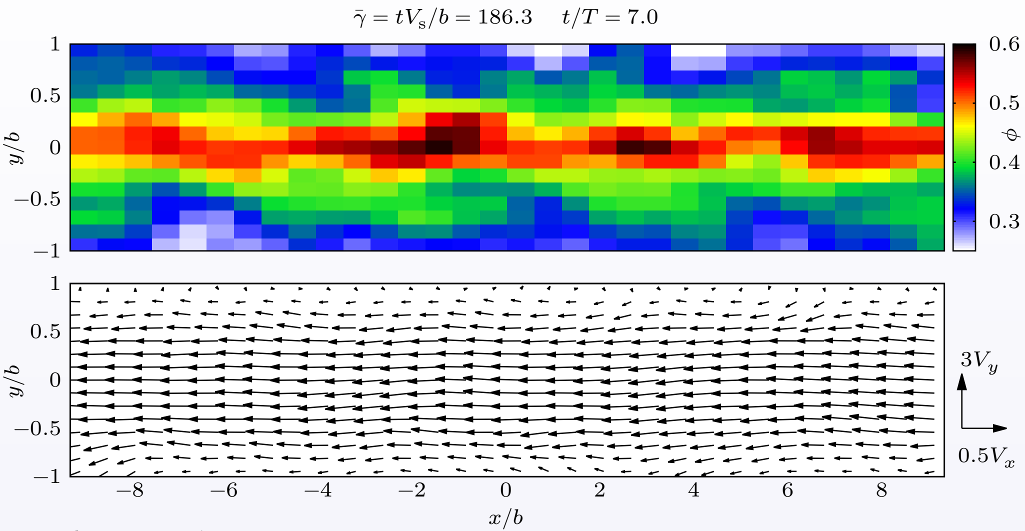


$2a = 85\,\mu\text{m}$ $2b = 2\,\text{mm}$ $\phi_{\text{bulk}} = 0.4$

# Volume fraction and velocity fields in the $xy$ plane

$\bar{\gamma} = tV_s/b = 266.2 \quad t/T = 10.0$

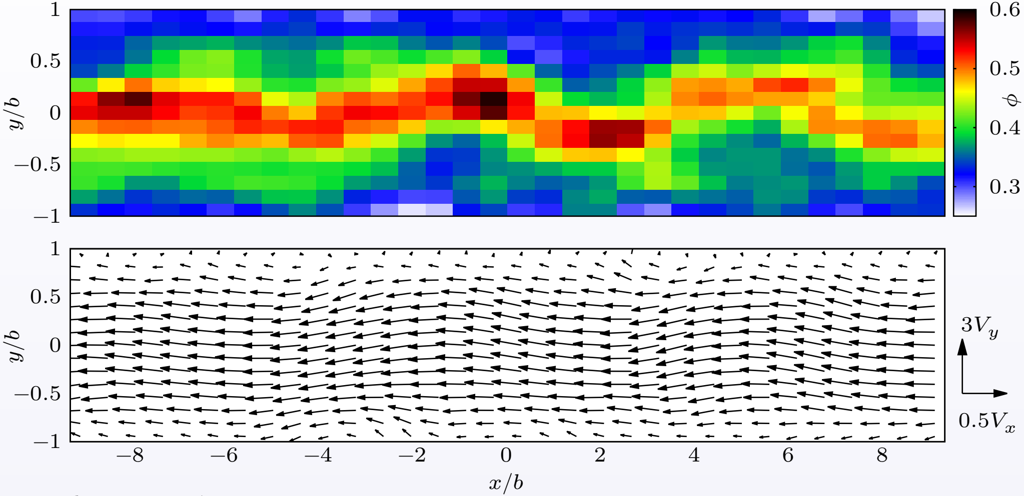


$2a = 85\,\mu m \quad 2b = 2\,mm \quad \phi_{bulk} = 0.4$

# Volume fraction and velocity fields in the $xy$ plane

$\bar{\gamma} = tV_s/b = 372.7 \quad t/T = 14.0$

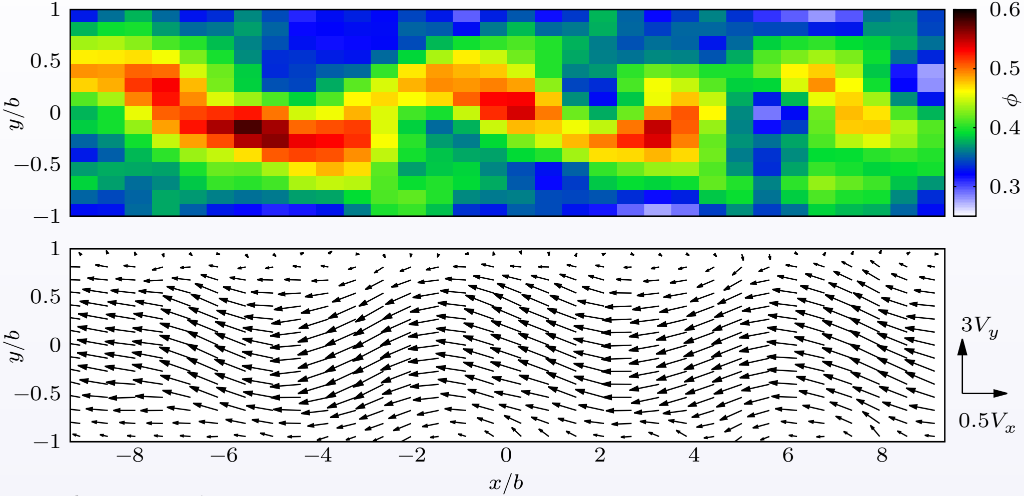


$2a = 85\,\mu\text{m} \quad 2b = 2\,\text{mm} \quad \phi_{\text{bulk}} = 0.4$

# Volume fraction and velocity fields in the $xy$ plane

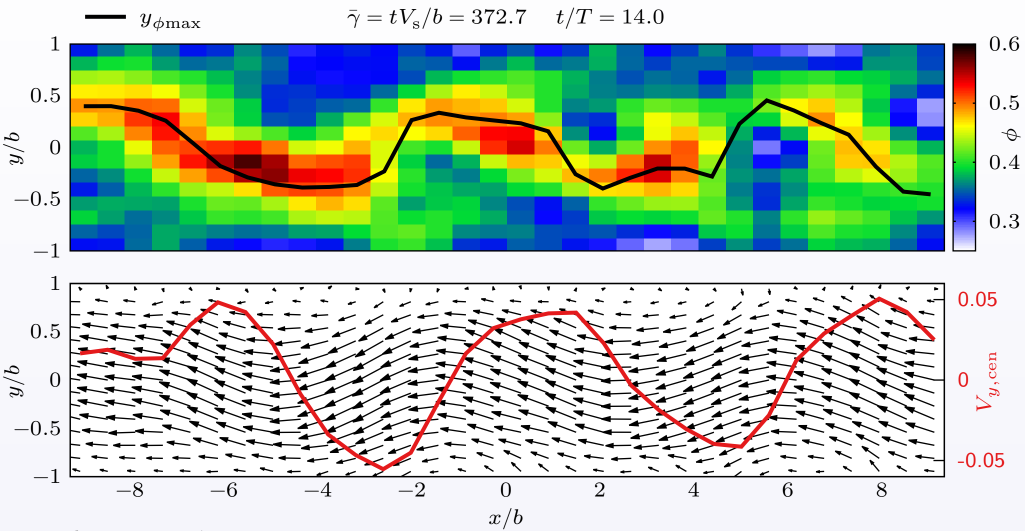


$2a = 85\,\mu m$ $2b = 2\,mm$ $\phi_{bulk} = 0.4$

# Secondary velocity field in the flow-gradient plane

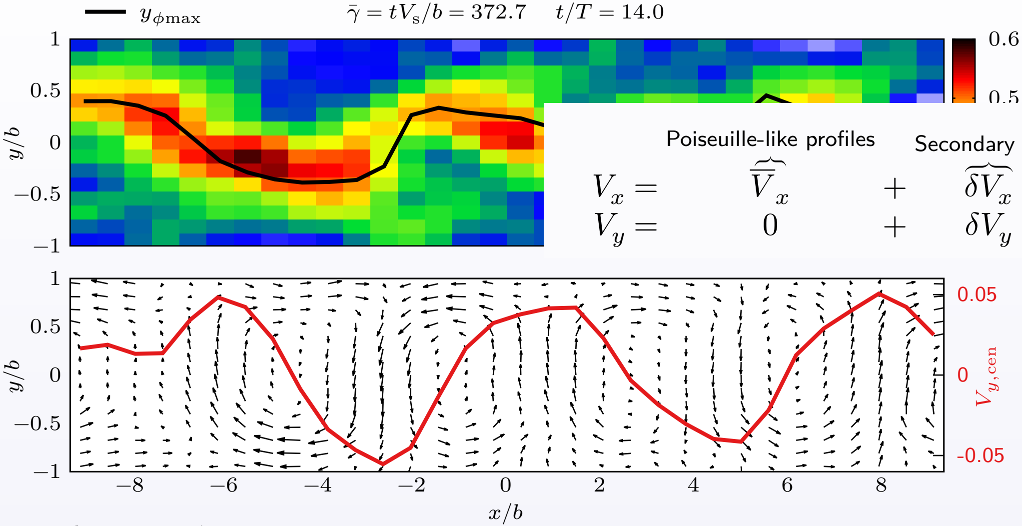


Poiseuille-like profiles | Secondary flow

$$V_x = \overbrace{\overline{V}_x} + \overbrace{\delta V_x}$$

$$V_y = 0 + \delta V_y$$

$2a = 85\,\mu\mathrm{m}$ $2b = 2\,\mathrm{mm}$ $\phi_{\mathrm{bulk}} = 0.4$

# Reversal and convection of the patterns

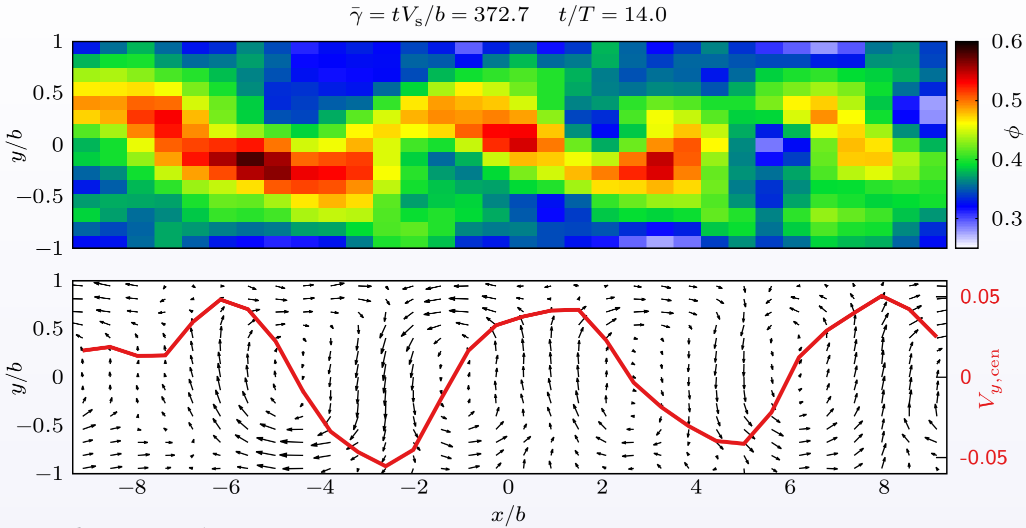


$2a = 85\,\mu m \quad 2b = 2\,mm \quad \phi_{\text{bulk}} = 0.4$

# Reversal and convection of the patterns

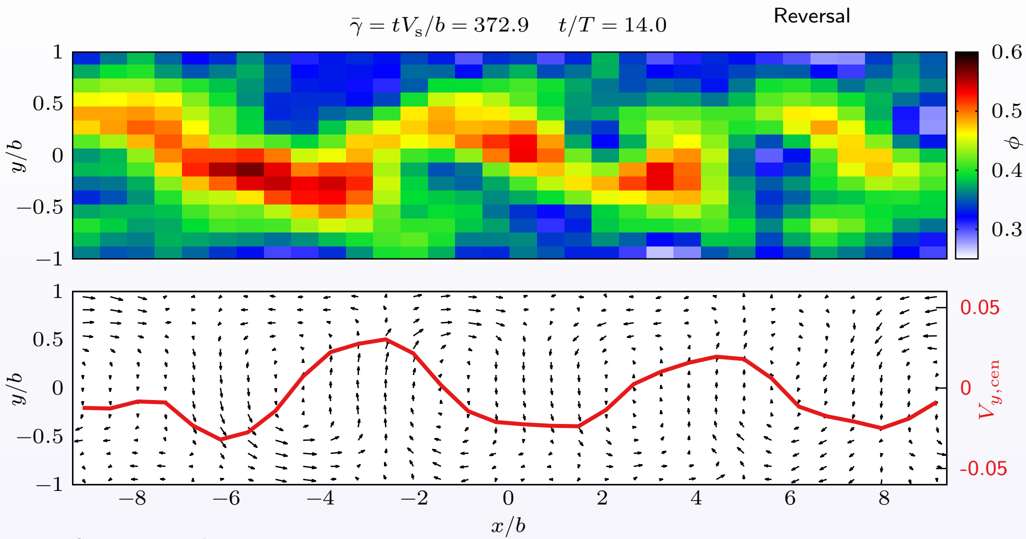


$2a = 85\,\mu m$ $2b = 2\,mm$ $\phi_{bulk} = 0.4$

# Reversal and convection of the patterns

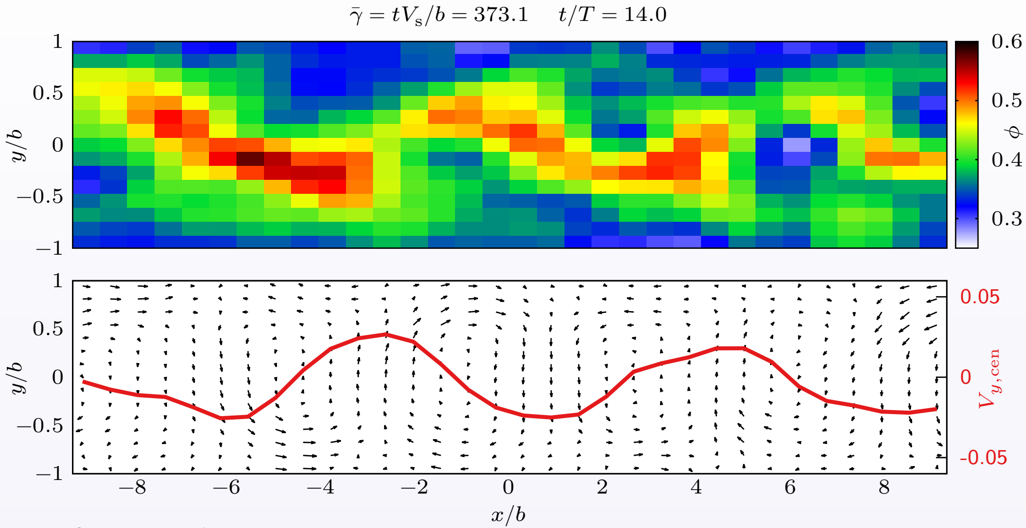


$2a = 85\,\mu\mathrm{m}$ $2b = 2\,\mathrm{mm}$ $\phi_{\mathrm{bulk}} = 0.4$

# Reversal and convection of the patterns

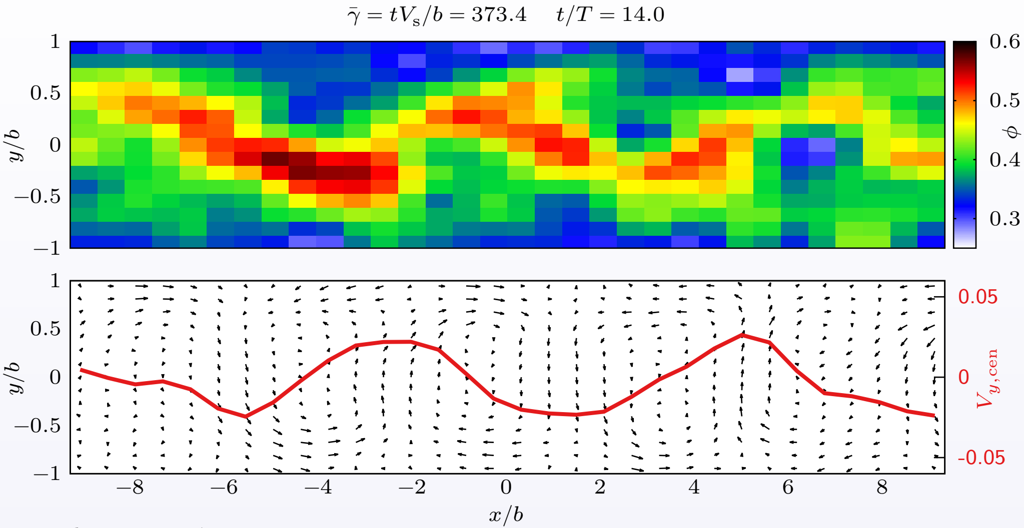


$2a = 85\,\mu\text{m} \quad 2b = 2\,\text{mm} \quad \phi_{\text{bulk}} = 0.4$

# Reversal and convection of the patterns

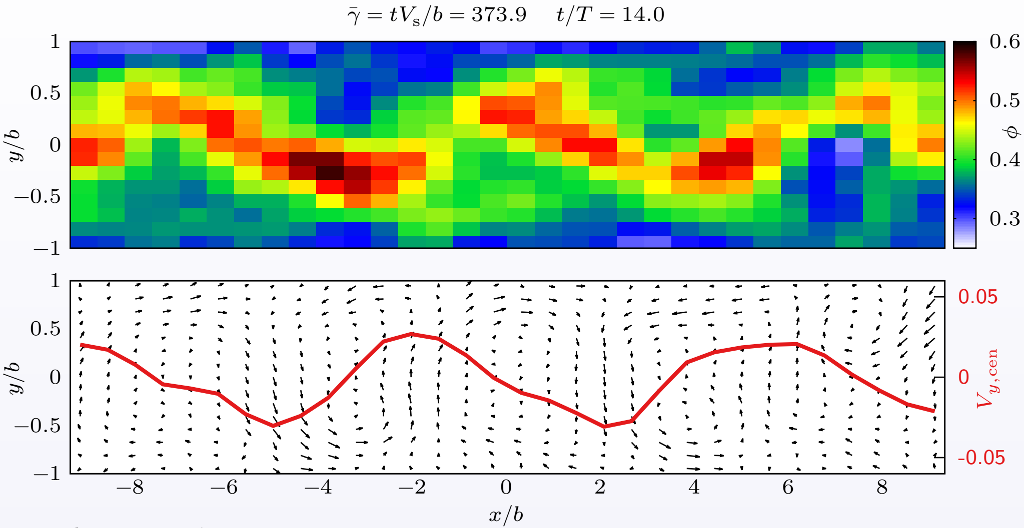


$2a = 85\,\mu\text{m}$ $2b = 2\,\text{mm}$ $\phi_{\text{bulk}} = 0.4$

# Reversal and convection of the patterns

$\bar{\gamma} = tV_s/b = 374.5 \quad t/T = 14.1$

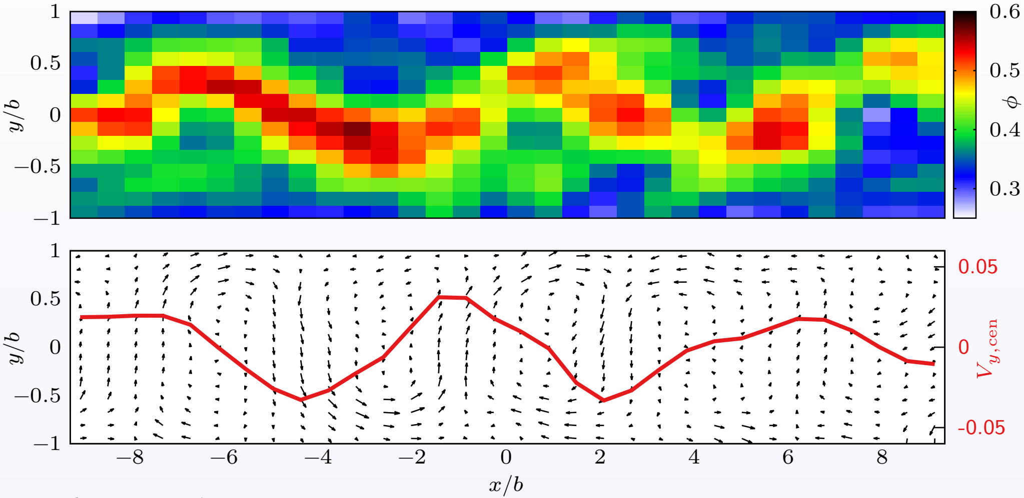


$2a = 85\,\mu\mathrm{m} \quad 2b = 2\,\mathrm{mm} \quad \phi_{\mathrm{bulk}} = 0.4$

# Reversal and convection of the patterns

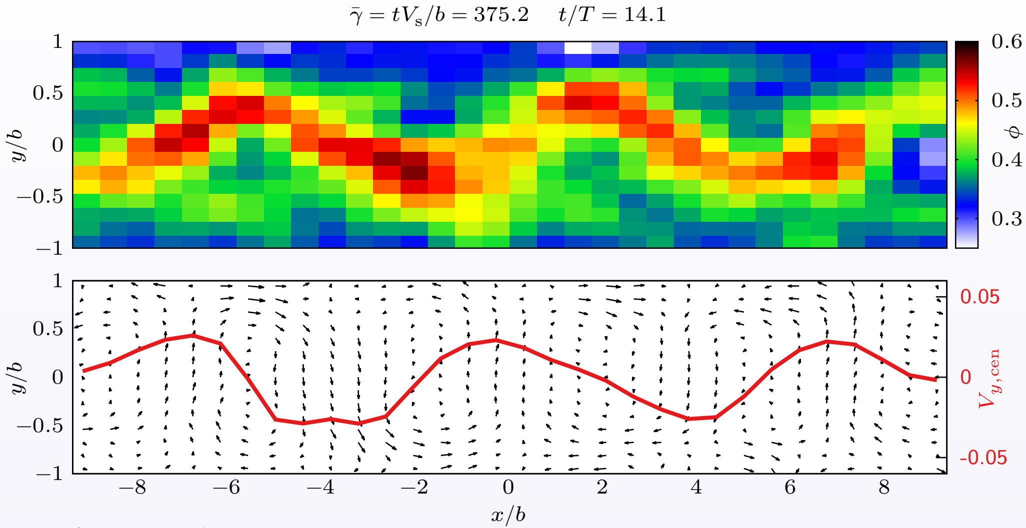


$2a = 85\,\mu\text{m} \quad 2b = 2\,\text{mm} \quad \phi_{\text{bulk}} = 0.4$

# Reversal and convection of the patterns

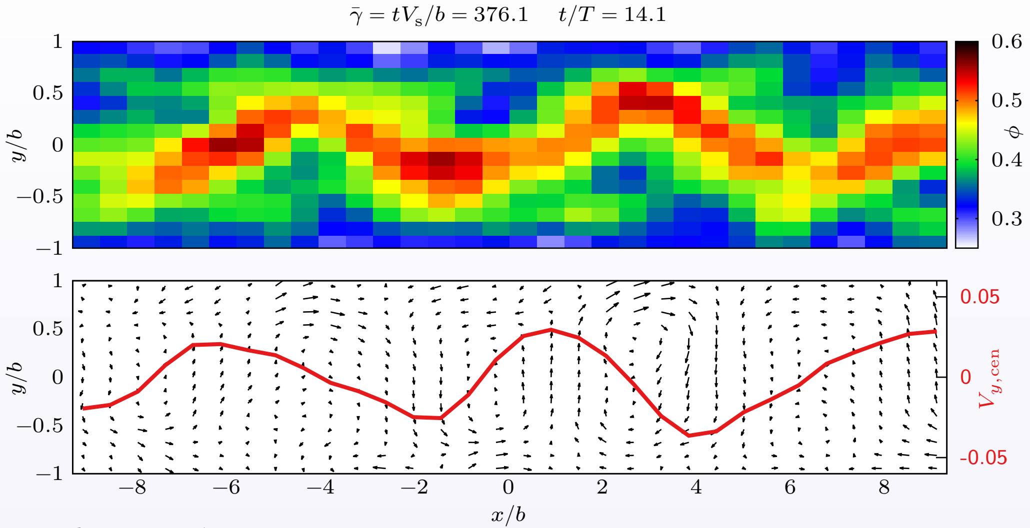


$2a = 85\,\mu\mathrm{m} \quad 2b = 2\,\mathrm{mm} \quad \phi_{\mathrm{bulk}} = 0.4$

# Reversal and convection of the patterns

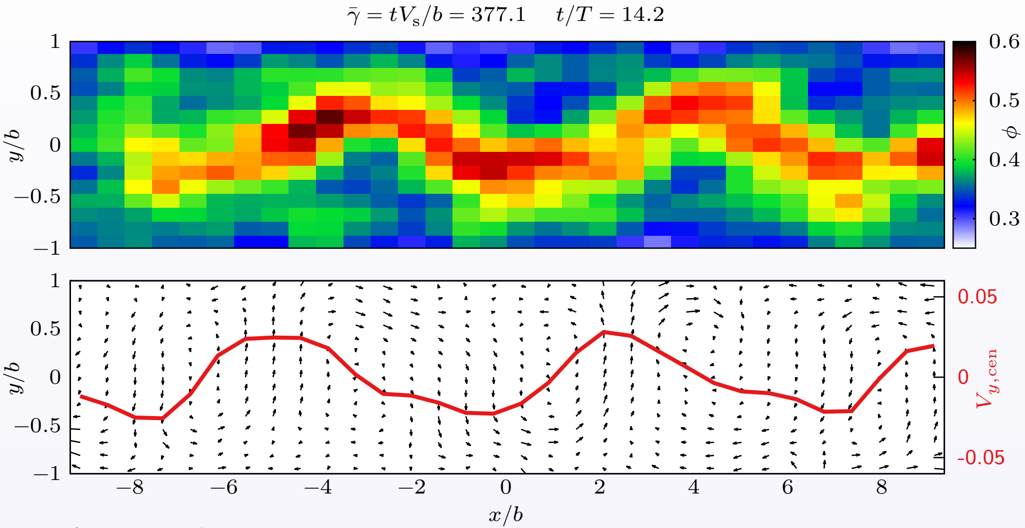


$2a = 85\,\mu\mathrm{m} \quad 2b = 2\,\mathrm{mm} \quad \phi_{\mathrm{bulk}} = 0.4$

# Reversal and convection of the patterns

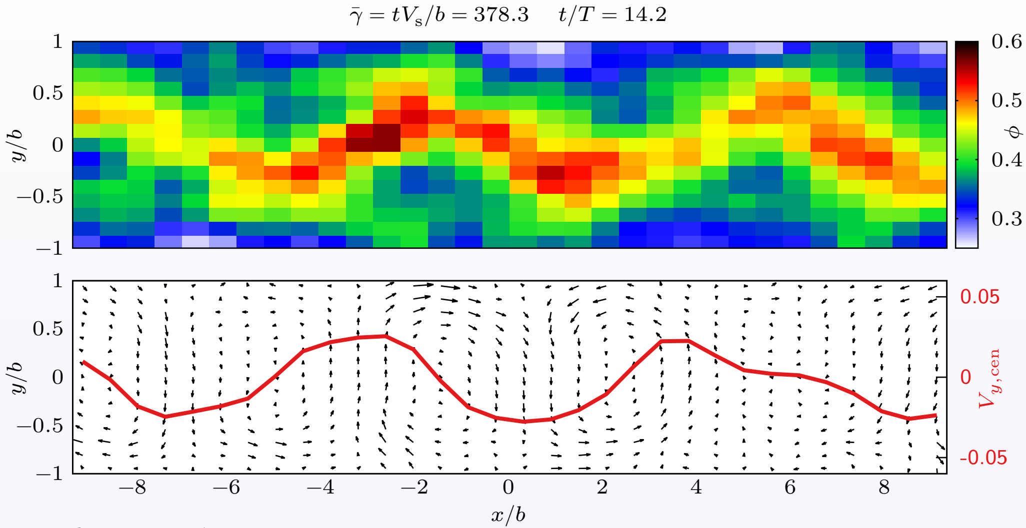


$2a = 85\,\mu\text{m}$ $2b = 2\,\text{mm}$ $\phi_{\text{bulk}} = 0.4$

# Reversal and convection of the patterns

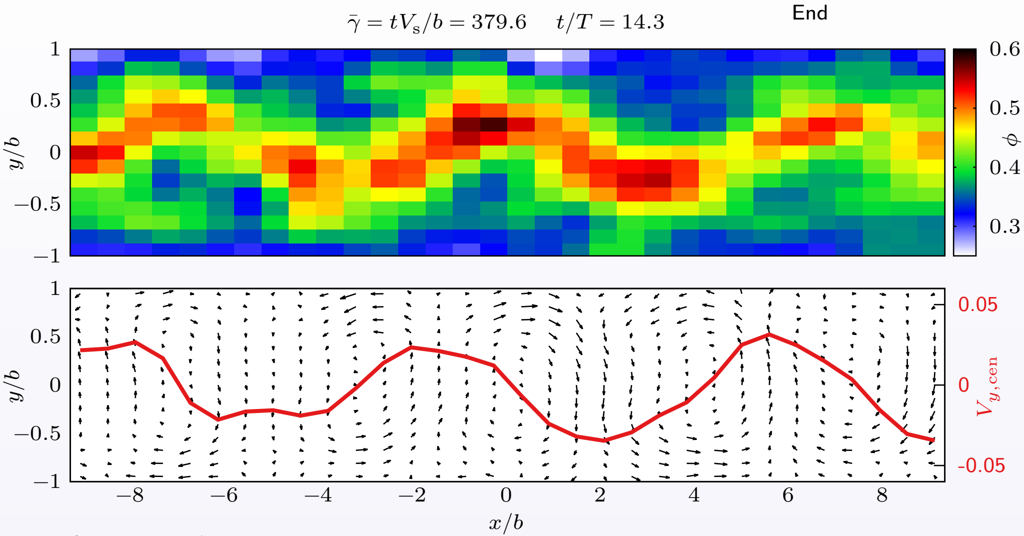


$2a = 85\,\mu\mathrm{m}$ $2b = 2\,\mathrm{mm}$ $\phi_{\mathrm{bulk}} = 0.4$

# Long-term evolution of key variables

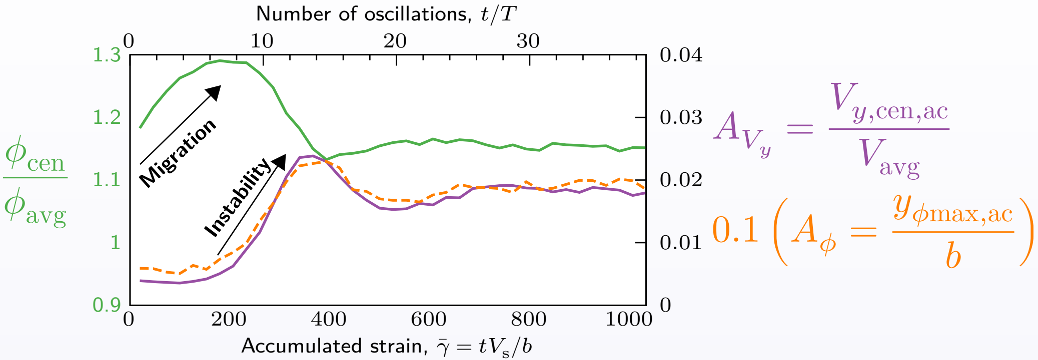


- One point per period, only quasi-steady state information.
- $\phi_{\mathrm{cen}}$: particle volume fraction near $y = 0$.
- $A_{V_y}$: normalized amplitude of the secondary flow.
- $A_\phi$: normalized amplitude of the deformation of the central band.

# Long-term evolution of key variables

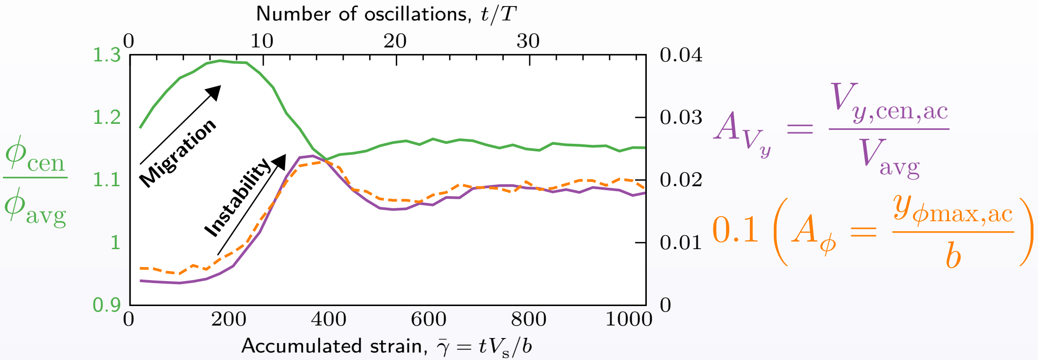


- One point per period, only quasi-steady state information.
- $\phi_{\text{cen}}$: particle volume fraction near $y = 0$.
- $A_{V_y}$: normalized amplitude of the secondary flow.
- $A_\phi$: normalized amplitude of the deformation of the central band.

Further characterization using $A_{V_y}(\bar{\gamma})$

# Influence of the oscillation amplitude for 85 µm particles

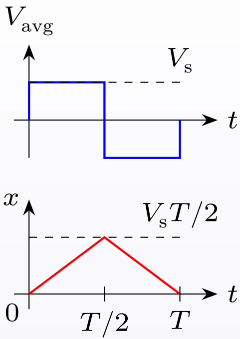


Accumulated strain:

$$\bar{\gamma} = \frac{V_s}{b} t$$

Oscillation amplitude:

$$\bar{\gamma}_0 = \frac{V_s}{b} \frac{T}{2}$$

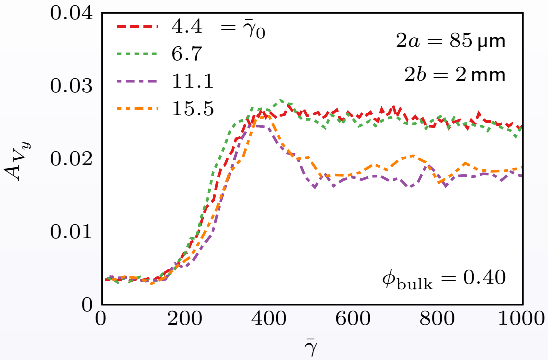


- The instability develops with similar strains $\bar{\gamma}$ in this range of $\bar{\gamma}_0$.
- Different $\bar{\gamma}_0 \Rightarrow$ different number of oscillations to reach a given $\bar{\gamma}$.

# Influence of the oscillation amplitude for 40 μm particles

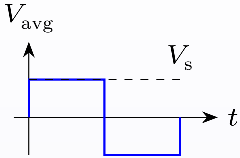


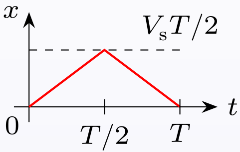


Accumulated strain:

$$\bar{\gamma} = \frac{V_{\text{s}}}{b} t$$

Oscillation amplitude:

$$\bar{\gamma}_0 = \frac{V_{\text{s}}}{b} \frac{T}{2}$$

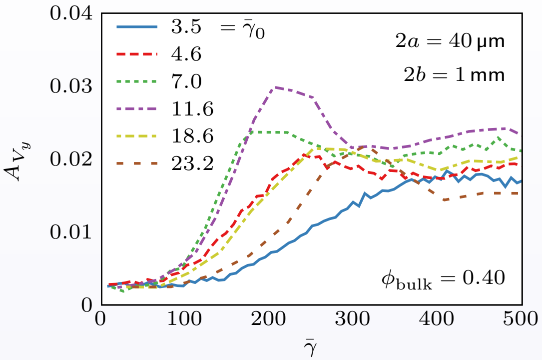


- Similar ratio $b/a \approx 25$, wider range of amplitudes $\bar{\gamma}_0$.
- Slower growth for extreme amplitudes.
- In general, faster than the 85 μm particles.

# Influence of the oscillation amplitude for 40 µm particles

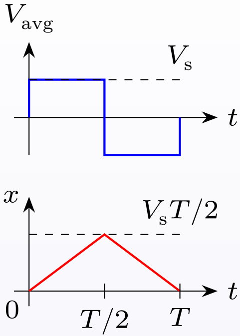


Accumulated strain:

$$\bar{\gamma} = \frac{V_s}{b} t$$

Oscillation amplitude:

$$\bar{\gamma}_0 = \frac{V_s}{b} \frac{T}{2}$$

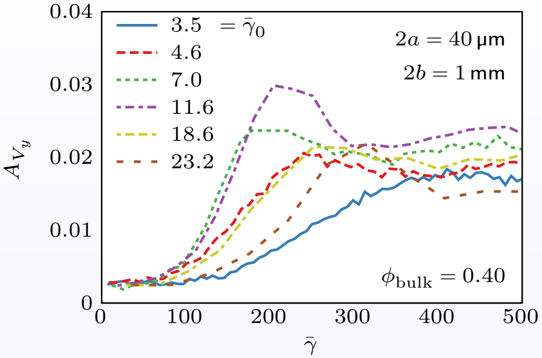


- Similar ratio $b/a \approx 25$, wider range of amplitudes $\bar{\gamma}_0$.
- Slower growth for extreme amplitudes.
- In general, faster than the 85 µm particles.

Maybe a difference in the asperity size?

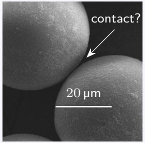

# Determination of the onset strain and a growth rate

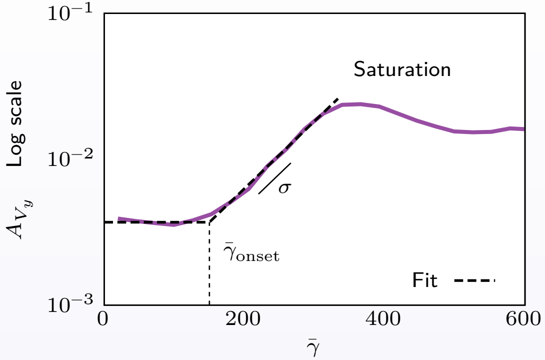


- Fit to $\log(A_{V_y})$ of a piecewise function: constant - linear - constant.
- The perturbations become apparent above a global strain $\bar{\gamma}_{\text{onset}}$.
- Then, they grow by a factor $\sigma$ per unit of strain.

# Onset strain and growth rate vs oscillation amplitude

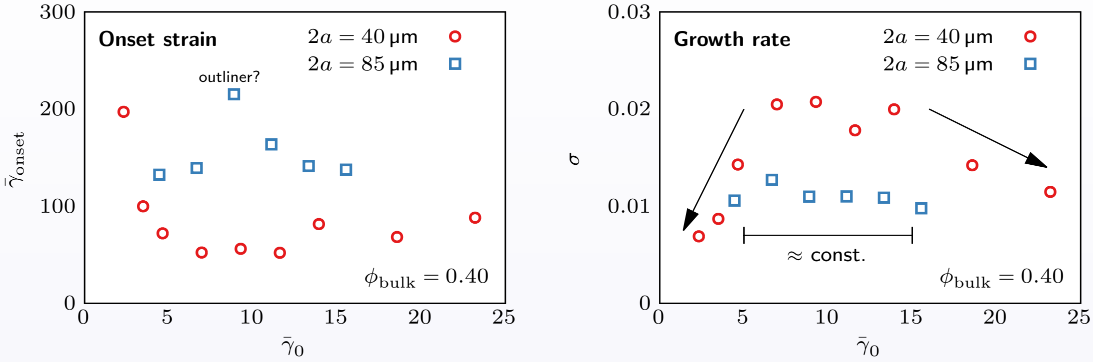


- $5 < \bar{\gamma}_0 < 15$: $\approx$ constant grow rates $\gamma$ and onset strains $\bar{\gamma}_{onset}$ (both sizes).
- $\bar{\gamma}_0 < 5$: delayed onset and reduced growth ($40\,\mu m$).
- $\bar{\gamma}_0 > 15$: delayed onset? and reduced growth ($40\,\mu m$).

# Onset strain and growth rate vs oscillation amplitude

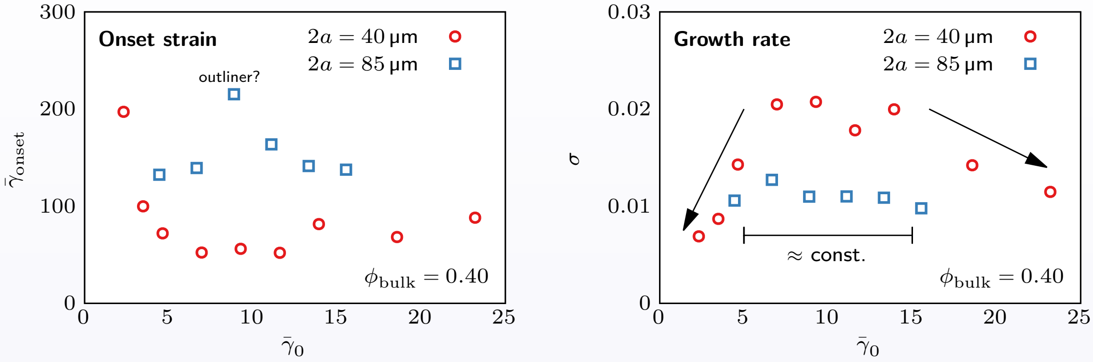


- $5 < \bar{\gamma}_0 < 15$: ≈ constant grow rates $\gamma$ and onset strains $\bar{\gamma}_{onset}$ (both sizes).
- $\bar{\gamma}_0 < 5$: delayed onset and reduced growth ($40\,\mu m$). ← Why?
- $\bar{\gamma}_0 > 15$: delayed onset? and reduced growth ($40\,\mu m$).

# Interpretation of the measured growth rates

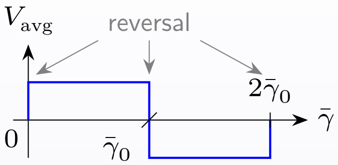


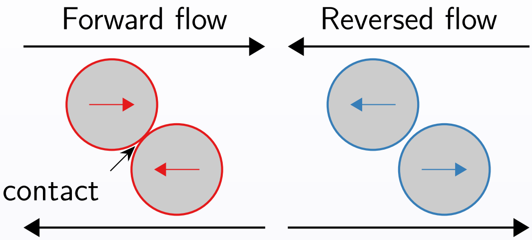


- Particle contacts → irreversible behavior → instability.
- After reversal, particles lose contacts...
- ...and recover them after accumulating a strain $\gamma_c \sim 1$.

# Interpretation of the measured growth rates

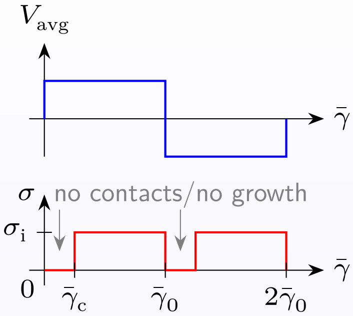


Effective growth rate during one half oscillation:

$$\sigma = \frac{\bar{\gamma}_0 - \bar{\gamma}_c}{\bar{\gamma}_0}\,\sigma_i$$

# Interpretation of the measured growth rates

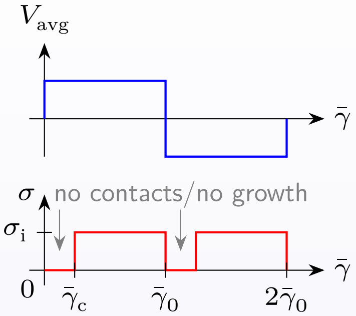


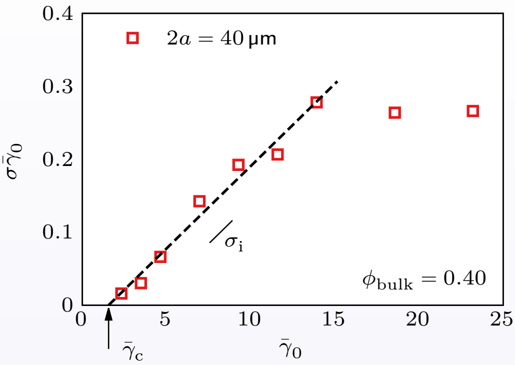


Effective growth rate during one half oscillation:

$$\sigma = \frac{\bar{\gamma}_0 - \bar{\gamma}_{\mathrm{c}}}{\bar{\gamma}_0}\,\sigma_{\mathrm{i}}$$

$\sigma\bar{\gamma}_0$: growth factor during one half oscillation.

- $\bar{\gamma}_0 < \bar{\gamma}_{\mathrm{c}}$: no growth. $\bar{\gamma}_{\mathrm{c}}$ is a threshold.
- $\bar{\gamma}_0 > 15$: another process?

# Influence of the particle volume fraction

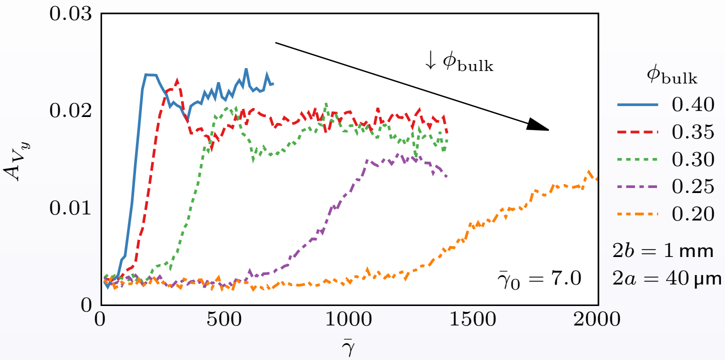


- Lower particle concentration
  $\rightarrow$ Lower collision rate
  $\rightarrow$ Slower progress in irreversible processes.
- Slight decrease of the maximum amplitude.

# Influence of the particle volume fraction

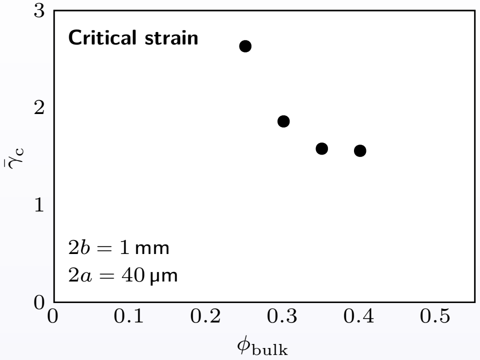


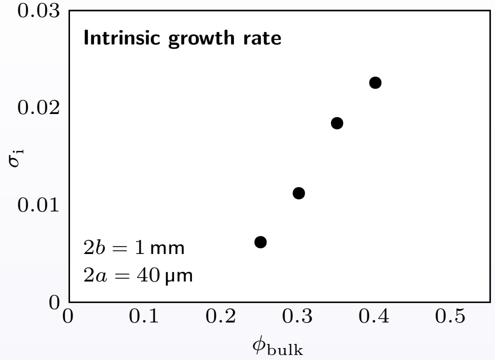


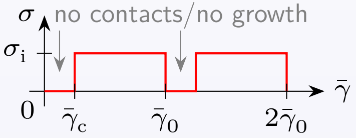


- $\bar{\gamma}_c$ decreases with $\phi_{bulk}$.
  The characteristic strain for microstructure reorganization decreases with $\phi$ (local).
- $\sigma_i$ increases with $\phi_{bulk}$,
  maybe like the particle diffusivity.

# Summary

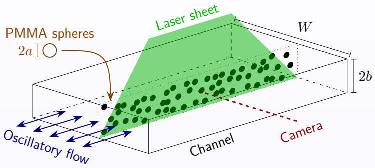


- Experiments with oscillating suspensions inside narrow channels (Hele-Shaw cells). Re $\approx 0$.
- Tracking of individual particles.
- Instability characterized by perturbations of the particle concentration and velocity fields periodic along the flow direction.

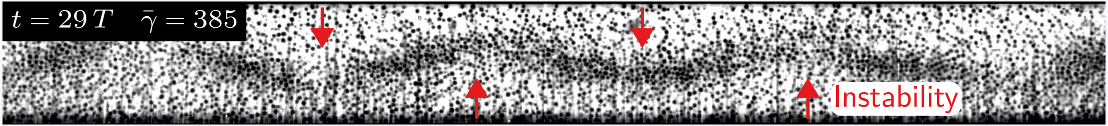

# Summary

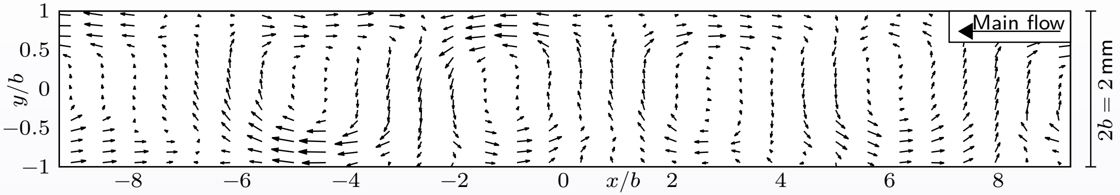


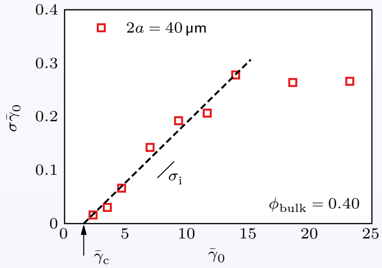


- The instability induces alternating recirculation rolls, convected and reversed by the main flow.
- The amplitude of this secondary flow grows $\approx$ exponentially with a rate $\sigma$.
- Threshold oscillation amplitude $\bar{\gamma}_c \sim 1$ due to the loss of particle contacts after each reversal.

# Summary

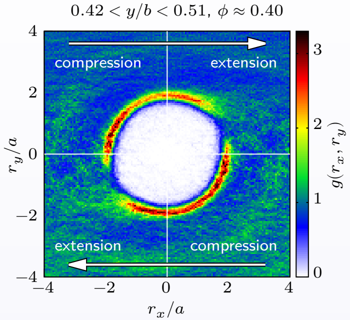


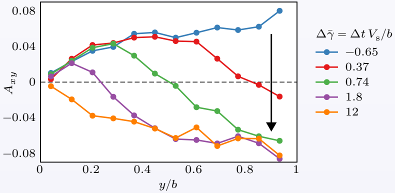


- Microstructure: particle pairs in compression are more common than in extension (steady regime).
- After reversal, the microstructure reorganizes after accumulating a local strain $\gamma \sim 1$.
- The microstructure influences properties like the normal stresses.
- Its transient and inhomogeneous variations after reversal may be the keys to explain the instability.

# Thanks

To my thesis directors/supervisors:


Irene IPPOLITO

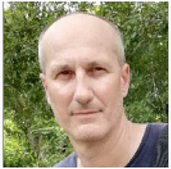
Georges GAUTHIER


Lucrecia ROHT

To my collaborators:


Jean-Pierre HULIN


Dominique SALIN


German DRAZER

To the members of the jury.

And to everyone for their attention!